Clim. Past Discuss., 11, 5651–5681, 2015
www.clim-past-discuss.net/11/5651/2015/
doi:10.5194/cpd-11-5651-2015

Climate of the Past Discussions

The South American Monsoon Variability over the Last Millennium in CMIP5/PMIP3 simulations

M. Rojas[1,2], **P. A. Arias**[3,1], **V. Flores-Aqueveque**[2], **A. Seth**[4], **and M. Vuille**[5]

[1]Department of Geophysics, University of Chile, Santiago, Chile
[2]Millennium Nucleus PaleoClimate, Santiago, Chile
[3]Grupo de Ingeniería Gestión Ambiental (GIGA), Escuela Ambiental, Facultad de Ingeniería, Universidad de Antioquia, Medellín, Colombia
[4]Department of Geography, University of Connecticut, Storrs, USA
[5]Department of Atmospheric and Environmental Sciences, University at Albany, Albany, USA

Received: 8 November 2015 – Accepted: 15 November 2015 – Published: 8 December 2015

Correspondence to: M. Rojas (maisa@dgf.uchile.cl)

Published by Copernicus Publications on behalf of the European Geosciences Union.

Abstract

In this paper we assess South American Monsoon System (SAMS) variability throughout the Last Millennium as depicted by the Coupled Modelling Intercomparison Project version 5/Paleo Modelling Intercomparison Project version 3 (CMIP5/PMIP3) simulations. High-resolution proxy records for the South American monsoon over this period show a coherent regional picture of a weak monsoon during the Medieval Climate Anomaly period and a stronger monsoon during the Little Ice Age (LIA). Due to the small forcing during the past 1000 years, CMIP5/PMIP3 model simulations do not show very strong temperature anomalies over these two specific periods, which in turn do not translate into clear precipitation anomalies, as suggested by rainfall reconstructions in South America. However, with an ad-hoc definition of these two periods for each model simulation, several coherent large-scale atmospheric circulation anomalies were identified. The models feature a stronger Monsoon during the LIA associated with: (i) an enhancement of the rising motion in the SAMS domain in austral summer, (ii) a stronger monsoon-related upper-troposphere anticyclone, (iii) activation of the South American dipole, which results to a certain extent in a poleward shift in the South Atlantic Convergence Zone and (iv) a weaker upper-level sub tropical jet over South America, this providing important insights into the mechanisms of these climate anomalies over South America during the past millennium.

1 Introduction

It is well established that monsoon systems respond to orbital forcing (Kutzbach and Liu, 1997; Kutzbach et al., 2007; Bosmans et al., 2012). At orbital timescale (especially related to the precessional cycle of approx. 19 and 21 ka), changes in the latitudinal insolation gradient, and hence temperatures, force the monsoon circulation globally (e.g., Bosmans et al., 2012). Because at the pace of the precessional cycle the summer insolation in both hemispheres is in anti-phase (for example, when Northern Hemisphere

(NH) summer insolation is at its maximum, summertime insolation in the Southern Hemisphere (SH) is at its minimum), it weakens the monsoonal circulation and precipitation in the SH summer monsoon systems and enhances it in the NH, or vice versa. The mechanism for the orbital-induced monsoon variability is therefore mainly related to latitudinal temperature gradients. In view of this mechanism, it is not surprising that other phenomena that produce important changes in hemispheric temperature gradients are also responsible for monsoon variability, as for example the abrupt Dansgaard–Oeschger events during the last glacial (Kanner et al., 2012; Cheng et al., 2013) and Heinrich events, including the Heinrich 1 event, during the last deglaciation (ca. 17 ka BP) (e.g., Griffiths et al., 2013; Deplazes et al., 2014; Cruz et al., 2006; Strikis et al., 2015).

In recent years, similar variability has also been observed for shorter timescales, in particular between the two most prominent climate anomalies over the Last Millennium (LM), namely the Medieval Climate Anomaly (MCA, ca. 950–1250 CE) and the Little Ice Age (LIA, ca. 1450–1850 CE) (e.g., Masson-Delmotte et al., 2013). Various recent high-resolution records from the area of the South American Monsoon System (SAMS) have been used to reconstruct precipitation over this region. Records include speleothems (Novello et al., 2012; Kanner et al., 2013; Apaestegui et al., 2014), pollen (Ledru et al., 2013), lake sediments (Bird et al., 2011), as well as tree-ring reconstructions (Morales et al., 2012). Vuille et al. (2012) reviews current available proxy records for the SAMS region. Most reconstructions show good correlations with NH temperature and Intertropical Convergence Zone (ITCZ) reconstructions. According to these paleoclimate studies, the LIA was characterized by a cool north equatorial Atlantic and a warm south equatorial Atlantic (Haug et al., 2001; Polissar et al., 2006) whereas an opposite pattern was present during the MCA. This meridional thermal gradient led to a southward (northward) migration of the Atlantic ITCZ during the LIA (MCA) (Haug et al., 2001). A second suggested mechanism for a southward (northward) migration of the ITCZ near South America during LIA (MCA) is given by paleoclimate reconstructions and modelling studies that identify an increased prevalence of El Niño-like (La

Niña-like) temperature anomalies in the eastern tropical Pacific through the LIA (MCA) period (Cobb et al., 2003; Mann et al., 2009; Salvatteci et al., 2014). Such a southward (northward) migration of the regional ITCZ would favor enhanced (reduced) rainfall over the Amazon and SAMS region during the LIA (MCA) (e.g., Cohen et al., 2009). Indeed, SAMS reconstructions during the last millennium show a weaker monsoon during the MCA period and a relatively stronger monsoon during the LIA period (e.g. Bird et al., 2011; Vuille et al., 2012; Ledru et al., 2013; Apaestegui et al., 2014), indicating an anti-correlation with reconstructions of the Southeast Asian monsoon (Zhang et al., 2008; Shi et al., 2014; Polanski et al., 2014), as well as with the North African and North American monsoons (Asmerom et al., 2013), for those periods.

Moreover, modelling studies support the suggestion of a southward (northward) shift of the Atlantic ITCZ during LIA (MCA) derived from temperature and precipitation reconstructions. For instance, model simulations presented by Vellinga and Wu (2004) suggest that anomalous northward ocean heat transports during MCA are linked to an enhanced cross-equatorial temperature gradient in the Atlantic and a northward movement of the ITCZ. Kageyama et al. (2013) analyzed fresh water hosing simulations over the North Atlantic to force fluctuations of the Atlantic Meridional Overturning Circulation. Their analyses suggest that the model response to an enhanced fresh water flux in the region is characterized by a general cooling of the North Atlantic, a southward shift of the Atlantic ITCZ, and a weakening of the African and Indian monsoons. Furthermore, the modelling experiments discussed by Broccoli et al. (2006) and Lee et al. (2011) indicate that when cooler-than-normal temperatures are imposed in the North Atlantic, as those occurred during the LIA, the Atlantic ITCZ shifts southward, strengthening the northern Hadley cell in austral summer and shifting its rising branch slightly southward. Thus, different paleoclimate reconstruction and modelling approaches suggest then that the particular temperature anomalies observed during the MCA and LIA periods, especially in the North Atlantic, could modify the location of the ITCZ in South America, affecting the strength of the summer SAMS throughout the past millennium (see also a review by Schneider et al., 2014).

Recent experiments simulating climate over the LM (850–1850 CE) have been incorporated into the third phase of the Paleoclimate Modelling Intercomparison Project (PMIP3). About a dozen of current CMIP5 models run this experiment, which considers solar, volcanic, greenhouse gases, and land use scenarios during the LM (Schmidt et al., 2011, 2012). In this paper, we explore to what extent the CMIP5/PMIP3 LM simulations capture the variability of the SAMS associated with LIA and MCA temperature anomalies, as suggested by rainfall reconstructions and diverse modelling studies in the region. This evaluation provides further insights on the response of the current generation of General Circulation Models (GCMs) to forcing during the LM. We focus on the models' ability of simulating the variability of the main feature of the South American climate during two periods of near-global temperature anomalies. This paper is organized as follows: Sect. 2 presents a short description of the model simulations considered and the methodology used to identify the MCA and LIA periods; Sect. 3 presents the main results from the CMIP5/PMIP3 simulations of the SAMS during both periods; and Sect. 4 presents a discussion and the main conclusions from this study.

2 Methodology and model simulations

We used nine available CMIP5/PMIP3 model LM simulations, as indicated in Table 1. These simulations cover the period 850–1850 CE, although some of them have been continued up to the present. Since not all modeling groups have continuous runs to the present (including the period 1850–2000) available, the analysis in this paper covers only the period until 1850 CE. The LM simulations have been forced with orbital variations (mainly shifts in the perihelion date), common solar irradiance, two different volcanic eruption reconstructions, land-use change, and greenhouse gas (GHG) concentrations. A full description of the exact forcings used in these LM simulations is given by Schmidt et al. (2011, 2012). Furthermore, a detailed list of individual forcings applied in each simulation is given in Annex 2 of Masson-Delmotte et al. (2013).

2.1 Definition of periods

In the fifth Intergovernmental Panel on Climate Change (IPCC) assessment report (AR5) (IPCC, 2013), the two periods of most prominent climate anomalies over the past millennium were defined as between ca. 950–1250 CE for the MCA, and between ca. 1450–1850 CE for the LIA. This report also concludes that the MCA was a period of relative global warmth, although in general less homogenous than the current warmth, whereas the LIA was a much more globally uniform cold period (Masson-Delmotte et al., 2013). Furthermore, a recent analysis of the consistency of the CMIP5/PMIP3 LM temperature simulations indicates that these simulations often differ from available temperature reconstructions in their long-term multi-centennial trends, which is related to the transition from the MCA to the LIA period (Bothe et al., 2013). Figure 1a shows the NH temperature anomaly time series for each of the nine models considered, as well as its ensemble mean. For comparison, the average of three NH temperature reconstructions (Hegerl et al., 2009; D'Arrigo et al., 2006; Ljungqvist, 2010) is shown. From the figure it is clear that the temperature anomalies over the last millennium are small, and that there is not a clearly common identifiable MCA and LIA. In particular for the MCA this is consistent with the idea that this climate anomaly is mostly result of internal climate variability.

Therefore, we decided to identify these two periods individually in each model. We used two criteria for the identification of the periods. First, for each model, the warmest (MCA) and coldest (LIA) periods between 850 and 1850 CE were defined by calculating the annual temperature anomaly over the NH (north of 30° N) with respect to the 1250–1450 mean (a period in between the MCA and LIA). Secondly, given the evidence for Atlantic southward/northward shifts of the ITCZ related to sea surface temperature gradient between the tropical north and south Atlantic, we also calculated the surface temperature gradient between the box (5–20° N) and (20–5° S) in the Atlantic, which again resulted in small values, maximum gradients of 0.5 °C. Finally, the periods were selected when both criteria were met. For example for the LIA, we choose the period with cold NH temperature anomalies coinciding with cold temperature anomalies in the North Atlantic box colder that that its South Atlantic box counterpart (negative gradient, not shown). The MCA and LIA periods identified in each model are shown in Table 1. Note that in general the periods are of the order of 80–110 years long, shorter than the more general MCA and LIA definition. Figure 1b shows the Gaussian fit of the frequency distribution of all the years defined as LIA years (red curve) and MCA years (blue curve). The two periods are statistically significantly different (*t* test, 5 % significance level). Because of the small anomaly values, we also calculated if both periods are significantly different from the mean of their respectively control simulation (piControl), and again the differences resulted significantly different at the 5 % significance level. In addition, Fig. 2 shows the maps of the annual mean temperature anomalies during LIA and MCA, as well as their difference, for the ensemble mean. Temperature anomalies in the models are largest over the NH and in particular over the North Atlantic domain. Importantly, however, the LIA and MCA periods identified in the models are not synchronous, as shown in Table 1.

2.2 Variables used

To identify the main differences in LM simulations of the SAMS, particularly during the LIA and MCA periods, we analyzed monthly CMIP5/PMIP3 output for rain rate, and 850 and 200 hPa horizontal winds. In addition, the local Hadley Cell was evaluated using the meridional mass streamfunction (Ψ), which is computed from zonal mean meridional wind [v] over the American sector (80–30° W, 35° S–15° N). Here, Ψ is defined as the vertically integrated northward mass flux at latitude φ from pressure level p to the top of the atmosphere. Thus,

$$\Psi(\phi, p) = \frac{2\pi\cos\phi}{g}\int_0^p [v(\phi, p)]\mathrm{d}p \qquad (1)$$

Title Page
Abstract | Introduction
Conclusions | References
Tables | Figures
◀| |▶
◀ ▶
Back | Close
Full Screen / Esc
Printer-friendly Version
Interactive Discussion

where g denotes the acceleration due to gravity. All the calculations were carried out from monthly mean values, from which climatological means were calculated, and seasonal and annual means evaluated.

The oceanic Inter-tropical Convergence Zone (ITCZ) was identified as the tropical latitude with the maximum precipitation, at all longitudes over the ocean. For this the precipitation was first interpolated into a much higher grid of 0.1°.

The next section examines the performance of the models and to what extent they simulate a stronger SAMS during the LIA, in comparison to the MCA, as suggested by precipitation proxies and previous modelling experiments. In addition, since the SAMS is a dominant feature of the South American climate during austral summer (e.g., Vera et al., 2006), we focused on its mature phase, the December–January–February (DJF) season.

3 Simulated SAMS circulation

3.1 Precipitation

Figure 3a shows the annual mean precipitation difference between the LIA and MCA periods, including the climatological precipitation of the reference period in dashed contours. Blue and red curves correspond to the annual mean position of the oceanic ITCZ during LIA and MCA periods, respectively. The ensemble mean shows that the precipitation differences are small and statistically significant only in some regions (t test, $p < 0.05$). There is more precipitation during LIA compared with the MCA in Northeastern Brazil and across the Atlantic, both regions that are directly affected by the ITCZ position in current climate. The mean position of the ITCZ between the two periods does not show any significant shifts (see Fig. 3b), but a small southward shift in the Atlantic during LIA is found, in accordance with the precipitation signal. Individually, models do show at some longitudes (Pacific and Atlantic Oceans) that during LIA, the ITCZ was shifted further southward, when compared with the MCA (not shown).

Figure 4a shows climatological precipitation and 850 hPa atmospheric circulation over the SAMS region during austral summer. In general, models are able to reproduce the main summer circulation and precipitation features over South America observed in present day climate. Particularly, a narrow oceanic ITCZ, a broad area of maxima rainfall over the continent (SAMS), and a southeast-northwest oriented South Atlantic convergence zone (SACZ) are observed in LM simulations, as shown by present-day observations (e.g., Garreaud et al., 2009); however, some models exhibit a double ITCZ over the eastern Pacific. This bias has been previously identified in CMIP3 and CMIP5 simulations, especially during austral summer and fall seasons (Hirota and Takayabu, 2013; Sierra et al., 2015). Despite the limitations of model resolution, austral summer lower tropospheric circulation simulated by the ensemble mean reproduces a cyclonic circulation over southeastern Bolivia (a.k.a. "Chaco low") and its associated northerly low-level jet, which is channeled by the Andes topography, transporting moisture to southern South America (Marengo et al., 2004).

When comparing LIA and MCA composites for DJF (Fig. 4b), models exhibit an increased easterly flow over northern South America (more southwards) and a stronger northerly low-level jet north of the Chaco low region, which would be consistent with a stronger summer SAMS during the LIA period. Models also simulate less summer SAMS precipitation during LIA over the Amazon and the SACZ, but more in the Nordeste. The pattern over the Amazon and the SACZ is in opposition to rainfall reconstructions in the region inAmazon and SACZ as well as Nordeste (e.g., Vuille et al., 2012; Novello et al., 2012). By contrast, when considering annual mean simulations (Fig. 3), most models show a southward migration of the Atlantic ITCZ (not very visible in the ensemble mean) and enhanced precipitation over the SAMS domain during the LIA, particularly over the eastern and southern Amazon, in agreement with paleoclimatological records for this period. This indicates that CMIP5/PMIP3 LM simulations are not able to reproduce the expected changes of the austral summer Atlantic ITCZ location and SAMS rainfall during LIA and MCA periods. The positive changes in the annual mean seen in Fig. 3 are due to the spring and autumn transition seasons.

Title Page
Abstract Introduction
Conclusions References
Tables Figures
◀| |▶
◀ ▶
Back Close
Full Screen / Esc
Printer-friendly Version
Interactive Discussion

3.2 Local Hadley cell

Several studies indicate that the strong seasonality of the SAMS is partially induced by the meridional migration of the local Hadley Cell (e.g., Trenberth et al., 2000; Dima and Wallace, 2003). Modelling results from Lee et al. (2011) suggest that the southward shift of the Atlantic ITCZ during a colder NH event strengthens the northern Hadley cell in austral summer, shifting its rising branch slightly southward into South America. Thus, to identify if CMIP5/PMIP3 LM simulations exhibit coherent anomalies in the local Hadley Cell over the American sector (80–30° W, 35° S–15° N) during LIA and MCA periods, we analyzed the climatological DJF meridional mass streamfunction estimated from CMIP5/PMIP3 winds for both periods (Fig. 5). In general, models reproduce the main local austral summer Hadley Cell characteristics: a stronger branch located over the winter hemisphere (NH) with enhanced rising motion over the SH, mainly between 10° S and the equator, and a weaker branch over the summer hemisphere (SH). The local Hadley Cell during the LIA is somewhat more intense compared with the MCA, especially in the descending part in the NH, and to a smaller extent in the ascending part over the SH, but there is no significant latitudinal shift of the cell (see Fig. 5b). This is only partially in agreement with the modelling experiment by Lee et al. (2011).

The intensification of the Hadley cell upward branch over South America, shown by most models during the LIA, is consistent with the enhanced precipitation as suggested by rainfall reconstructions in the region for this period (e.g., Vuille et al., 2012), although this pattern is not borne out in the corresponding rainfall simulated by these models.

3.3 Bolivian high and subtropical jet

The well-documented southward migration of the Hadley Cell and its rising center from 10° N in JJA to 10° S in DJF is only a part of the monsoon rainfall seasonal migration over the Americas, which reaches a more southward location in austral summer (Dima and Wallace, 2003). Furthermore, this wide area of continental convection, although related to local convergence zones, is not only a result of the shift of the ITCZ into subtropical latitudes. The establishment of the Bolivian high, the characteristic monsoon upper-level anticyclone located over the central Andes during austral summer, and the position and strength of the SH subtropical jet (SHSJ) in South America are also related to this monsoonal convective activity (Lenters and Cook, 1997; Garreaud et al., 2003; Yin et al., 2014).

To identify changes in the Bolivian high during the LM, we analyzed the austral summer upper-troposphere circulation during the LIA and MCA (Fig. 6). Results indicate a stronger and more southeastward location of the SAMS anticyclone during the LIA. This strengthening of the Bolivian high is consistent with a stronger SAMS circulation. The southward shift of this upper-level anticyclone is related to an enhanced summer easterly flow over the central Andes, as suggested by previous studies (Lenters and Cook, 1999), and in turn would favor moisture transport and rainfall over the region (Garreaud et al., 2003). Moreover, the upper tropospheric wind anomalies strikingly resemble the South American dipole (e.g. Robertson and Mechoso, 2000), a primary mode of variability over this region. An anticyclonic anomaly is associated with a diffuse SACZ, enhancing moisture convergence and precipitation on its southwestern flank (i.e. leading to a poleward shift in the location of the SACZ). Again, model simulations do not show this enhanced austral summer rainfall in the Amazon and central Andes during the LIA, and feature only marginally more precipitation to the southwest (Fig. 3).

On the other hand, recent studies have identified that the strength and location of the SHSJ, which corresponds to the southward extent of the Hadley Cell, is a key factor for triggering convection during the dry-to-wet season transition in the Amazon (Yin et al., 2014). Particularly, when the SHSJ is weaker and/or reaches a more equatorward location, it favors the incursion of synoptic disturbances to subtropical South America (e.g., Garreaud, 2000), enhancing lower-troposphere convergence and triggering the wet season onset over the region (e.g., Li and Fu, 2006). To identify simulated changes of the SHSJ during the LIA and the MCA, Fig. 7 shows the 30 $\mathrm{m\,s^{-1}}$ isotach of the climatological September–November 200 hPa zonal wind as well as the difference between LIA and MCA periods. In general, the ensemble mean does not exhibit significant changes in the SHSJ location over South America during either period, as also indicated by Fig. 6b; however, the models simulate a weaker SHSJ during the LIA, not only at the annual mean, but also during the austral spring and summer seasons (not shown). This weaker SHSJ, particularly during austral spring (i.e., the transition season from dry to wet conditions in the SAMS), would allow a stronger influence of cold air incursions to trigger SAMS convection and probably maintain a stronger monsoon during the LIA.

4 Discussion and conclusions

According to our analysis, CMIP5/PMIP3 LM simulations are able to identify circulation features coherent with a stronger SAMS during the LIA: (i) an enhancement of the rising motion in the SAMS domain in austral summer, (ii) a stronger monsoon-related upper-troposphere anticyclone, (iii) activation of the South American dipole, which results to a certain extent in a poleward shift in the SACZ and (iv) a weaker spring SHSJ over South America. However, austral summer simulations do not exhibit the expected increase in precipitation in this region during this cold period, as suggested by proxy evidence, except over Nordeste, where it is not expected based on proxy data (e.g., Bird et al., 2011; Vuille et al., 2012; Ledru et al., 2013; Apaestegui et al., 2014). Furthermore, CMIP5/PMIP3 LM simulations only reproduce a slight, but insignificant, southward (northward) shift of the austral summer Atlantic ITCZ during the LIA (MCA), unlike results found in other modeling studies (Vellinga and Wu, 2004; Lee et al., 2011; Kageyama et al., 2013). This meridional shift of the Atlantic ITCZ has been typically considered to explain the changes of SAMS rainfall observed during these periods (e.g., Vuille et al., 2012).

Recent studies indicate that the new generation of models included in the Coupled Model Intercomparison Project Phase 5 (CMIP5) still tend to perform poorly in simulating precipitation in South America, especially over the Amazon basin, and the Atlantic

ITCZ (Yin et al., 2013; Siongco et al., 2014; Sierra et al., 2015). However, CMIP5 models have shown further improvement in simulating precipitation over the region, in comparison to the CMIP3 generation (Jones and Carvalho, 2013; Yin et al., 2013; Hirota and Takayabu, 2013).

What could bias the simulated austral summer SAMS rainfall response of the CMIP5/PMIP3 models during the past millennium? Recent studies indicate that CMIP5 simulations tend to overestimate rainfall over the Atlantic ITCZ (Yin et al., 2013) and exhibit either an East or West Atlantic bias, in association with overestimated rainfall along the African (Gulf of Guinea) or South American (Brazil) coasts, respectively (Siongco et al., 2014). Such a misinterpretation of the local ITCZ has been shown to bias rainfall simulations in the core of the SAMS (Bombardi and Carvalho, 2011). Particularly, a stronger Atlantic ITCZ may contribute to enhanced surface divergence over tropical South America, inducing drier conditions in the region (e.g., Li et al., 2006), as observed in CMIP5 historical simulations (Yin et al., 2013; Sierra et al., 2015). However, a stronger local ITCZ does not necessarily translate into reduced SAMS rainfall since moisture convergence in this region is mainly influenced by the SACZ (Vera et al., 2009). Thus, the weaker SACZ during the LIA simulated by these models (Fig. 3) could reduce moisture convergence and rainfall over the SAMS. Furthermore, positive feedbacks between land surface latent heat flux, rainfall, surface net radiation, and large-scale circulation are also found to contribute to the dry biases over the Amazon and SAMS in most of the CMIP5 historical simulations (Yin et al., 2013).

Another circulation feature related to SAMS rainfall is the intensity and location of the South Atlantic subtropical high. The eastward displacement of this anticyclone and its interaction with the SACZ provide favorable conditions for monsoon precipitation (Raia and Cavalcanti, 2008). Recent analysis of CMIP5 projections under different scenarios suggests that this surface anticyclone is likely to strengthen in association with globally warmer conditions (Li et al., 2013). Thus, a detailed examination of the response of this subtropical high to LM forcing is necessary in order to provide further explanations for

Title Page
Abstract | Introduction
Conclusions | References
Tables | Figures
◀| |▶
◀ ▶
Back | Close
Full Screen / Esc
Printer-friendly Version
Interactive Discussion

the inadequate CMIP5/PMIP3 simulations of the SAMS rainfall variability throughout the past millennium.

The previous generation of LM model simulations reproduced warmer temperatures during the MCA when compared with the LIA, but generally underestimated the regional changes detected from available reconstructions or failed to simulate a synchronous response in accordance with these reconstructions (e.g., Gonzalez-Rouco et al., 2011). The latter has been mainly related to uncertainties in the forcing estimates, as well as reduced sensitivity to external perturbations, underestimated internal variability, or incorrect representation of important feedbacks in GCMs (e.g. Goosse et al., 2005; Braconnot et al., 2012). Furthermore, a recent model simulation of the global monsoons during the LM, performed in a non PMIP3-experiment, indicates that the NH summer monsoon responds more sensitively to GHG forcing than the SH monsoon rainfall, which appears to be more strongly influenced by solar and volcanic forcing (Liu et al., 2012). Hence, a stronger sensitivity of SAMS rainfall to LM forcing estimations and the inadequate response of current GCMs to such forcing may also bias the CMIP5/PMIP3 simulations of the summer SAMS rainfall during the past millennium. Particularly, the small temperature anomalies simulated by these models during the MCA (Figs. 1 and 2) could contribute to the inadequate changes of austral summer rainfall in South America between LIA and MCA (Figs. 3 and 4).

The evaluation of CMIP5/PMIP3 simulations of the SAMS throughout the past 1000 years presented here confirms previous findings regarding the ability of the current generation of GCMs to reproduce large-scale circulation features in South America and their lack of an adequate representation of precipitation over the region. The availability of precipitation reconstructions from South America has been useful to provide new insights into the GCMs response to past forcing. However, the weak or absent temperature and precipitation response to the imposed forcing in climate models provides a formidable challenge for proxy-model comparisons. To better compare and eventually reconcile model reconstructions with proxy evidence will require a more detailed analysis of precipitation-generating mechanisms in climate models. Our results indicate that the CMIP5/PMIP3 models quite accurately reproduce changes in the large-scale circulation that are consistent with proxy evidence over the past millennium. These changes, however, do not translate into corresponding precipitation changes. This implies that the models may lack relevant feedbacks or that precipitation in the models may be too dependent on the microphysics and convective parameterization schemes, but not sufficiently sensitive to large-scale circulation mechanisms. On the proxy side, a stronger effort to not only reconstruct surface climate at individual locations, but also focus on reconstructions of modes of variability or entire climate components such as the SAMS, which implicitly include circulation changes, are needed. Proxies such as pollen or stable hydrogen and oxygen isotopes from lakes, speleothems and ice cores have shown potential to record larger-scale climate signals and changes in the tropical hydrological cycle over South America (Vuille and Werner, 2005; Vimeux et al., 2009; Bird et al., 2011; Vuille et al., 2012; Ledru et al., 2013; Flantua et al., 2015; Hurley et al., 2015). Multi-proxy reconstructions from such networks, which implicitly incorporate remote and large-scale circulation aspects, may therefore provide a better tool to assess the performance of climate models than reconstructions that are based solely on local precipitation estimates.

Acknowledgements. We acknowledge the World Climate Research Programme's Working Group on Coupled Modeling, which is responsible for CMIP5, and we thank the climate modeling groups for producing and making available their model outputs. This work was partially funded by NC120066, FONDAP-CONICYT no. 15110009. MR acknowledges support from FONDECYT grant #1131055. PAA was supported by FONDECYT grant #3140570 and the Programme "Estrategia de Sostenibilidad 2014–2015" at Universidad de Antioquia, Colombia. V. Flores-Aqueveque acknowledges funding from FONDECYT grant #11121543. AS acknowledges financial support from NSF CAREER Award# 1056216 and NOAA grant NA11OAR4310109. M. Vuille was partially supported by NSF award AGS-1303828.

References

Apaéstegui, J., Cruz, F. W., Sifeddine, A., Vuille, M., Espinoza, J. C., Guyot, J. L., Khodri, M., Strikis, N., Santos, R. V., Cheng, H., Edwards, L., Carvalho, E., and Santini, W.: Hydroclimate variability of the northwestern Amazon Basin near the Andean foothills of Peru related to the South American Monsoon System during the last 1600 years, Clim. Past, 10, 1967–1981, doi:10.5194/cp-10-1967-2014, 2014.

Asmerom, Y., Polyak, V. J., Rasmussen, J. B. T., Burns, S. J., and Lachniet, M.: Multidecadal to multicentury scale collapses of Northern Hemisphere monsoons over the past millennium, P. Natl. Acad. Sci. USA, 110, 9651–9656, 2013.

Bao, Q., Lin, P., Zhou, T., Liu, Y., and coauthors: The flexible global ocean–atmosphere–land system model, spectral version: FGOALS-s2, Adv. Atmos. Sci., 30, 561–576, doi:10.1007/s00376-012-2113-9, 2012.

Bird, B. W., Abbott, M. B., Vuille, M., Rodbell, D. T., Stansell, N. D., and Rosenmeier, M. F.: a 2,300-year-long annually resolved record of the South American summer monsoon from the Peruvian Andes, P. Natl. Acad. Sci. USA, 108, 8583–8588, doi:10.1073/pnas.1003719108, 2011.

Bombardi, R. J. and Carvalho, L. M. V.: The South Atlantic dipole and variations in the characteristics of the South American Monsoon in the WCRP-CMIP3 multi-model simulations, Clim. Dynam., 36, 2091–2102, doi:10.1007/s00382-010-0836-9, 2011.

Bosmans, J. H. C., Drijfhout, S. S., Tuenter, E., Lourens, L. J., Hilgen, F. J., and Weber, S. L.: Monsoonal response to mid-holocene orbital forcing in a high resolution GCM, Clim. Past, 8, 723–740, doi:10.5194/cp-8-723-2012, 2012.

Bothe, O., Jungclaus, J. H., and Zanchettin, D.: Consistency of the multi-model CMIP5/PMIP3-past1000 ensemble, Clim. Past, 9, 2471–2487, doi:10.5194/cp-9-2471-2013, 2013.

Braconnot, P., Harrison, S. P., Kageyama, M., Bartlein, P. J., Masson-Delmotte, V., Abe-Ouchi, A., Otto-Bliesner, B., and Zhao, Y.: Evaluation of climate models using palaeoclimatic data, Nature Climate Change, 2, 417–424, doi:10.1038/nclimate1456, 2012.

Broccoli, A. J., Dahl, K. A., and Stouffer, R. J.: Response of the to Northern Hemisphere cooling,ITCZ, Geophys. Res. Lett., 33, L01702, doi:10.1029/2005GL024546, 2006.

Cheng, H., Sinha, A., Cruz, F. W., Wang, X., Edwards, R. L., d'Horta, F. M., Ribas, C. C., Vuille, M., Stott, L. D., and Auler, A. S.: Climate change patterns in Amazonia and biodiversity, Nature Commun., 4, 1411, doi:10.1038/ncomms2415, 2013.

Cobb, K. M., Charles, C. D., Cheng, H., and Edwards, R. L.: El Niño/Southern Oscillation and tropical Pacific climate during the last millennium, Nature, 424, 271–276, 2003.

Cohen, M. C. L., Behling, H., Lara, R. J., Smith, C. B., Matos, H. R. S., and Vedel, V.: Impact of sea-level and climatic changes on the Amazon coastal wetlands during the late Holocene, Veg Hist. Archaeobot., 18, 425–439, 2009.

Cruz Jr., F. W., Burns, S. J., Karmann, I., Sharp, W. D., and Vuille, M.: Reconstruction of regional atmospheric circulation features during the Late Pleistocene in subtropical Brazil from oxygen isotope composition of speleothems, Earth Planet. Sc. Lett., 248, 494–506, 2006.

D'Arrigo, R., Wilson, R., and Jacoby, G.: On the long-term context for late twentieth century warming, J. Geophys. Res., 111, D03103, doi:10.1029/2005JD006352, 2006.

Deplazes, G., Lückge, A., Stuut, J.-B. W., Pätzold, J., Kuhlmann, H., Husson, D., Fant, M., and Haug, G. H.: Weakening and strengthening of the Indian monsoon during Heinrich events and Dansgaard–Oeschger oscillations, Paleoceanography, 29, 99–114, doi:10.1002/2013PA002509, 2014.

Dermody, B. J., de Boer, H. J., Bierkens, M. F. P., Weber, S. L., Wassen, M. J., and Dekker, S. C.: A seesaw in Mediterranean precipitation during the Roman Period linked to millennial-scale changes in the North Atlantic, Clim. Past, 8, 637–651, doi:10.5194/cp-8-637-2012, 2012.

Dima, I. M. and Wallace, J. M.: On the seasonality of the Hadley cell, J. Atmos. Sci., 60, 1522–1527, 2003.

Dufresne, J.-L., Foujols, M.-A., Denvil, S., Caubel, A., Marti, O., Aumont, O., Balkanski, Y., Bekki, S., Bellenger, H., and coauthors: Climate change projections using the IPSL-CM5 Earth System Model: from CMIP3 to CMIP5, Clim. Dynam., 40, 2123–2165, 2013.

Flantua, S. G. A., Hooghiemstra, H., Vuille, M., Behling, H., Carson, J. F., Gosling, W. D., Hoyos, I., Ledru, M. P., Montoya, E., Mayle, F., Maldonado, A., Rull, V., Tonello, M. S., Whitney, B. S., and González-Arango, C.: Climate variability and human impact on the environment in South America during the last 2000 years: synthesis and perspectives, Clim. Past Discuss., 11, 3475–3565, doi:10.5194/cpd-11-3475-2015, 2015.

Garreaud, R., Vuille, M., and Clement, A.: The climate of the Altiplano: observed current conditions and mechanism of past changes, Palaeogeogr. Palaeocl., 194, 1–18, 2003.

Garreaud, R. D.: Cold air incursions over subtropical South America: mean structure and dynamics, Mon. Weather Rev., 128, 2544–2559, 2000.

Garreaud, R. D., Vuille, M., Compagnucci, R., and Marengo, J.: Present-day South American climate, Palaeogeogr. Palaeocl., 281, 180–195, 2009.

Gent, P. R., Gokhan Danabasoglu, L. J., Donner, M. M., Holland, E. C., Hunke, S. R., Jayne, D. M., Lawrence, R. B., Neale, P. J., Rasch, M., Vertenstein, P. H., Worley, Z.-L., and Yang, M.: The community climate system model version 4, J. Climate, 24, 4973–4991, 2011.

Giorgetta, M. A., Jungclaus, J., Reick, C. H. Legutke, S., Bader, J., Böttinger, M., Brovkin, V., Crueger, T., Esch, M., Fieg, K., Glushak, K., Gayler, V., Haak, H., Hollweg, H.-D., Ilyina, T., Kinne, S., Kornblueh, L., Matei, D., Mauritsen, T., Mikolajewicz, U., Mueller, W., Notz, D., Pithan, F., Raddatz, T., Rast, S., Redler, R., Roeckner, E., Schmidt, H., Schnur, R., Segschneider, J., Six, K. D., Stockhause, M., Timmreck, C., Wegner, J., Widmann, H., Wieners, K.-H., Claussen, M., Marotzke, J. and Stevens, B.: Climate and carbon cycle changes from 1850 to 2100 in MPI-ESM simulations for the Coupled Model Intercomparison Project phase 5, J. Adv. Model. Earth Syst., 5, 572–597, doi:10.1002/jame.20038, 2013.

Gonzalez-Rouco, F. J., Fernandez-Donado, L., Raible, C. C., Barriopedro, D., Luterbacher, J., Jungclaus, J. H., Swingedouw, D., Servonnat, J., Zorita, E., Wagner, S., and Ammann, C. M.: Medieval Climate Anomaly to Little Ice Age transition as simulated by current climate models, in: Medieval Climate Anomaly, edited by: Xoplaki, E., Fleitmann, D., Diaz, H., von Gunten, L., and Kiefer, T., PAGES International Project Office, Pages News, Bern, Switzerland, 19, 7–8, 2011.

Goosse, H., Crowley, T., Zorita, E., Ammann, C., Renssen, H., and Driesschaert, E.: Modelling the climate of the last millennium: what causes the differences between simulations?, Geophys. Res. Lett., 32, L06710, doi:10.1029/2005GL022368, 2005.

Goosse, H., Crespin, E., Dubinkina, S., Loutre, M.-F., Mann, M. E., Renssen, H., Sallaz-Damaz, Y., and Shindell, D.: The role of forcing and internal dynamics in explaining the "Medieval Climate Anomaly", Clim. Dynam., 39, 2847–2866, 2012.

Griffiths, M. L., Drysdale, R. N., Gagan, M. K., Hellstrom, J. C., Couchoud, I., Ayliffe, L. K., Vonhof, H. B., and Hantoro, W. S.: Australasian monsoon response to Dansgaard–Oeschger event 21 and teleconnections to higher latitudes, Earth Planet. Sc. Lett., 369–370, 294–304, 2013.

Haug, G. H., Hughen, K. A., Sigman, D. M., Peterson, L. C., and Röhl, U.: Southward migration of the intertropical convergence zone through the Holocene, Science, 293, 1304–1306, 2001.

Hegerl, G. C., Crowley, T. J., Allen, M., Hyde, W. T., Pollack, H. N., Smerdon, J., and Zorita, E.: Detection of human influence on a new, validated 1500-year temperature reconstruction, J. Climate, 20, 650–666, doi:10.1175/JCLI4011.1, 2007.

Hirota, N. and Takayabu, Y. N.: Reproducibility of precipitation distribution over the tropical oceans in CMIP5 multi-climate models compared to CMIP3, Clim. Dynam., 41, 2909–2920, 2013.

Hurley, J. V., Vuille, M., Hardy, D. R., Burns, S., and Thompson, L. G.: Cold air incursions, δ^{18}O variability and monsoon dynamics associated with snow days at Quelccaya Ice Cap, Peru, J. Geophys. Res., 120, 7467–7487, doi:10.1002/2015JD023323, 2015.

IPCC: Climate Change 2013: The Physical Science Basis Contribution of Working Group I to the Fifth Assessment Report of the Intergovernmental Panel on Climate Change, edited by: Stocker, T. F., Qin, D., Plattner, G.-K., Tignor, M., Allen, S. K., Boschung, J., Nauels, A., Xia, Y., Bex, V., and Midgley, P. M., Cambridge University Press, Cambridge, and New York, UK, NY, USA, 1535 pp., doi:10.1017/CBO9781107415324, 2013.

Jones, C. and Carvalho, L. M. V.: Climate change in the South American Monsoon System: present climate and CMIP5 projections, J. Climate, 26, 6660–6678, 2013.

Kageyama, M., Merkel, U., Otto-Bliesner, B., Prange, M., Abe-Ouchi, A., Lohmann, G., Ohgaito, R., Roche, D. M., Singarayer, J., Swingedouw, D., and X Zhang: Climatic impacts of fresh water hosing under Last Glacial Maximum conditions: a multi-model study, Clim. Past, 9, 935–953, doi:10.5194/cp-9-935-2013, 2013.

Kanner, L. C., Burns, S. J., Cheng, H., and Edwards, R. L.: High-latitude forcing of the South American Summer monsoon during the last glacial, Science, 335, 570–573, 2012.

Kanner, L. C., Burns, S. J., Cheng, H., Edwards, R. L., and Vuille, M.: High-resolution variability of the South American summer monsoon over the last seven millennia: insights from a speleothem record from the central Peruvian Andes, Quaternary Sci. Rev., 75, 1–10, 2013.

Kutzbach, J. E. and Liu, Z.: Response of the African Monsoon to orbital forcing and ocean feedbacks in the middle holocene science, 278, 440–443, 1997.

Kutzbach, J. E., Liu, X., Liu, Z., and Chen, G.: Simulation of the evolutionary response of global summer monsoons to orbital forcing over the past 280 000 years, Clim. Dynam., 30, 567–579, 2007.

Ledru, M.-P., Jomelli, V., Samaniego, P., Vuille, M., Hidalgo, S., Herrera, M., and Ceron, C.: The Medieval Climate Anomaly and the Little Ice Age in the eastern Ecuadorian Andes, Clim. Past, 9, 307–321, doi:10.5194/cp-9-307-2013, 2013.

Lee, S.-Y., Chiang, J. C. H., Matsumoto, K., and Tokos, K. S.: Southern Ocean wind response to North Atlantic cooling and the rise in atmospheric CO_2: modeling perspective and paleoceanographic implications, Paleoceanography, 26, PA1214, doi:10.1029/2010PA002004, 2011.

Lenters, J. D. and Cook, K. H.: On the origin of the Bolivian high and related circulation features of the South American climate, J. Atmos. Sci., 54, 656–677, 1997.

Lenters, J. D. and Cook, K. H.: Summertime precipitation variability over South America: role of the large-scale circulation, Mon. Weather Rev., 127, 409–431, 1999.

Li, W. and Fu, R.: Influence of cold air intrusions on the wet season onset over Amazonia, J. Climate, 19, 257–275, doi:10.1175/JCLI3614.1, 2006.

Li, W., Fu, R., and Dickinson, R. E.: Rainfall and its seasonality over the Amazon in the 21st century as assessed by the coupled models for the IPCC AR4, J. Geophys. Res., 111, doi:10.1029/2005jd006355, 2006.

Li, W., Li, L., Ting, M., Deng, Y., Kushnir, Y., Liu, Y., Lu, Y., Wang, C., and Zhang, P.: Intensification of the Southern Hemisphere summertime subtropical anticyclones in a warming climate, Geophys. Res. Lett., 40, 5959–5964, doi:10.1002/2013GL058124, 2013.

Liu, J., Wang, B., Yim, S. Y., Lee, J. Y., Jhun, J. G., and Ha, K. J.: What drives the global summer monsoon over the past millennium?, Clim. Dynam., 39, 1063–1072, 2012.

Ljungqvist, F. C.: A new reconstruction of temperature variability in the extra-tropical Northern Hemisphere during the last two millennia, Geograf. Ann. Phys. Geogr., 92, 339–351, doi:10.1111/j.1468-0459.2010.00399.x, 2010.

Mann, M., Zhang, Z., Rutherford, S., Bradley, R., Hughes, M., Shindell, D., Ammann, C., Falugevi, G., and Ni, F.: Global signatures and dynamical origins of the Little Ice Age and Medieval Climate Anomaly, Science, 326, 1256–1260, doi:10.1126/science.1177303, 2009.

Marengo, J., Soares, W., Saulo, C., and Nicolini, M.: Climatology of the LLJ east of the Andes as derived from the NCEP reanalyses, J. Climate, 17, 2261–2280, 2004.

Masson-Delmotte, V., Schulz, M., Abe-Ouchi, A., Beer, J., Ganopolski, A., González Rouco, J. F., Jansen, E., Lambeck, K., Luterbacher, J., Naish, T., Osborn, T., Otto-Bliesner, B., Quinn, T., Ramesh, R., Rojas, M., Shao, X., and Timmermann, A.: Information from paleoclimate archives, in: Climate Change 2013: The Physical Science Basis. Contribution of Working Group I to the Fifth Assessment Report of the Intergovernmental Panel on Climate Change, edited by: Stocker, T. F., Qin, D., Plattner, G.-K., Tignor, M., Allen, S. K., Boschung, J., Nauels, A., Xia, Y., Bex, V., and Midgley, P. M., Cambridge University Press, Cambridge, and New York, UK, NY, USA, 2013.

Morales, M. S., Christie, D. A., Villalba, R., Argollo, J., Pacajes, J., Silva, J. S., Alvarez, C. A., Llancabure, J. C., and Soliz Gamboa, C. C.: Precipitation changes in the South American Altiplano since 1300 AD reconstructed by tree-rings, Clim. Past, 8, 653–666, doi:10.5194/cp-8-653-2012, 2012.

Novello, V. F., Cruz, F. W., Karmann, I., Burns, S. J., Stríkis, N. M., Vuille, M., Cheng, H., Edwards, R. L., Santos, R. V., Frigo, E., and Barreto, E. A. S.: Multidecadal climate variability in Brazil's Nordeste during the last 3000 years based on speleothem isotope records, Geophys. Res. Lett., 39, L23706, doi:10.1029/2012GL053936, 2012.

Phipps, S. J., Rotstayn, L. D., Gordon, H. B., Roberts, J. L., Hirst, A. C., and Budd, W. F.: The CSIRO Mk3L climate system model version 1.0 – Part 1: Description and evaluation, Geosci. Model Dev., 4, 483–509, doi:10.5194/gmd-4-483-2011, 2011.

Polanski, S., Fallah, B., Befort, D. J., Prasad, S., and Cubasch, U.: Regional moisture change over India during the past Millennium: a comparison of multi-proxy reconstructions and climate model simulations, Global Planet. Change, 122, 176–185, 2014.

Polissar, P. J., Abbott, M. B., Wolfe, A. P., Bezada, M., Rull, V., and Bradley, R. S.: Solar modulation of Little Ice Age climate in the tropical Andes P. Natl. Acad. Sci. USA, 103, 8937–8942, 2006.

Raia, A. and Cavalcanti, I. F. A.: The life cycle of the South American Monsoon System, J. Climate, 21, 6227–6246, 2008.

Raddatz, T. J., Reick, C. H., Knorr, W., Kattge, J., Roeckner, E., Schnur, R., Schnitzler, K.-G., Wetzel, P., and Jungclaus, J.: Will the tropical land biosphere dominate the climate-carbon cycle feedback during the twenty first century?, Clim. Dynam., 29, 565–574, doi:10.1007/s00382-007-0247-8, 2007.

Robertson, A. W. and Mechoso, C. R.: Interannual and interdecadal variability of the South Atlantic convergence zone, Mon. Weather Rev., 128, 2947–2957, 2000.

Salvatteci, R., Gutiérrez, D., Field, D., Sifeddine, A., Ortlieb, L., Bouloubassi, I., Boussafir, M., Boucher, H., and Cetin, F.: The response of the Peruvian Upwelling Ecosystem to centennial-scale global change during the last two millennia, Clim. Past, 10, 715–731, doi:10.5194/cp-10-715-2014, 2014.

Schmidt, G. A., Jungclaus, J. H., Ammann, C. M., Bard, E., Braconnot, P., Crowley, T. J., Delaygue, G., Joos, F., Krivova, N. A., Muscheler, R., Otto-Bliesner, B. L., Pongratz, J., Shindell, D. T., Solanki, S. K., Steinhilber, F., and Vieira, L. E. A.: Climate forcing reconstructions for use in PMIP simulations of the last millennium (v1.0), Geosci. Model Dev., 4, 33–45, doi:10.5194/gmd-4-33-2011, 2011.

Schmidt, G. A., Jungclaus, J. H., Ammann, C. M., Bard, E., Braconnot, P., Crowley, T. J., Delaygue, G., Joos, F., Krivova, N. A., Muscheler, R., Otto-Bliesner, B. L., Pongratz, J., Shindell, D. T., Solanki, S. K., Steinhilber, F., and Vieira, L. E. A.: Climate forcing reconstructions for use in PMIP simulations of the Last Millennium (v1.1), Geosci. Model Dev., 5, 185–191, doi:10.5194/gmd-5-185-2012, 2012.

Schneider, T., Bishoff, T., and Haug, G. H.: Migrations and dynamics of the intertropical convergence zone, Nature, 513, 45–53, 2014.

Schurer, A., Tett, S. F. B., Mineter, M., and Hegerl, G. C.: Euroclim500 – Causes of Change in European Mean and Extreme Climate over the Past 500 years: HadCM3 Model Output from the Experiment, NCAS British Atmospheric Data Centre, ALL, http://http://catalogue.ceda.ac.uk/uuid/ (last access: May 2015), 2013.

Shi, F., Li, J., and Wilson, R. J. S.: A tree-ring reconstruction of the South Asian summer monsoon index over the past millennium, Sci. Reports, 4, 6739, doi:10.1038/srep06739, 2014.

Sierra, J. P., Arias, P. A., and Vieira, S. C.: Precipitation over Northern South America and its seasonal variability as simulated by the CMIP5 models, Adv. Meteorol., 2015, 1–22, doi:10.1155/2015/634720, 2015.

Siongco, A. C., Hohenegger, C., and Stevens, B.: The Atlantic ITCZ bias in CMIP5 models, Clim. Dynam., 45, 1169–1180, doi:10.1007/s00382-014-2366-3, 2015.

Strikis, N. M., Chiessi, C. M., Cruz, F. W., Vuille, M., Cheng, H., de Sousa Barreto, E. A., Mollenhauer, G., Kasten, S., Karmann, I., Edwards, R. L., Bernal, J. P., and dos Reis Sales, H.: Timing and structure of Mega-SACZ events during Heinrich Stadial 1, Geophys. Res. Lett., 42, 5477–5484, doi:10.1002/2015GL064048, 2015.

Trenberth, K. E., Stepaniak, D. P., and Caron, J. M.: The Global Monsoon as seen through the divergent atmospheric circulation, J. Climate, 13, 3969–3993, 2000.

Vellinga, M. and Wu, P.: Low-latitude freshwater influence on centennial variability of the Atlantic thermohaline circulation, J. Climate, 17, 4498–4511, 2004.

Vera, C., Higgins, W., Amador, J., Ambrizzi, T., Garreaud, R., Gochis, D., Gutzler, D., Lettenmaier, D., Marengo, J., Mechoso, C. R., Nogues-Paegle, J., Silva Diaz, P. L., and Zhang, C.: Towards a unified view of the American Monsoon System, J. Climate, 19, 4977–5000, 2006.

Vera, C. S., Gonzalez, P., and Silvestri, G.: About uncertainties in WCRP/CMIP3 climate simulations over South America, in: Proceedings of the 9th International Conference on Southern

Hemisphere Meteorology and Oceanography, Melbourne, Australia, 9–13 February, p. 10, 2009.

Vimeux, F., Ginot, P., Schwikowski, M., Vuille, M., Hoffmann, G., Thompson, L. G., and Schotterer, U.: Climate variability during the last 1000 years inferred from Andean ice cores: a review of recent results, Palaeogeogr. Palaeocl., 281, 229–241, doi:10.1016/j.palaeo.2008.03.054, 2009.

Vuille, M. and Werner, M.: Stable isotopes in precipitation recording South American summer monsoon and ENSO variability – observations and model results, Clim. Dynam., 25, 401–413, doi:10.1007/s00382-005-0049-9, 2005.

Wu, T. W., Yu, R. C., Zhang, F., Wang, Z., Dong, M., and Wang, L.: The Beijing climate center for atmospheric general circulation model: description and its performance for the present-day climate, Clim. Dynam., 34, 123–147, 2010.

Yin, L., Fu, R., Shevliakova, E., and Dickinson, R. E.: How well can CMIP5 simulate precipitation and its controlling processes over tropical South America?, Clim. Dynam., 41, 3127–3143, 2013.

Yin, L., Fu, R., Zhang, Y.-F., Arias, P. A., Fernando, D. N., Li, W., Fernandes, K., and Bowerman, A. R.: What controls the interannual variation of the wet season onsets over the Amazon?, J. Geophys. Res. Atmos., 119, 2314–2328, doi:10.1002/2013JD021349, 2014.

Yukimoto, S., Yoshimura, H., Hosaka, M., Sakami, T., Tsujino, H., Hirabara, M., Tanaka, T. Y., Deushi, M., Obata, A., Nkano, H., Adachi, Y., Shindo, E., Yabu, S., Ose, T., and Kitoh, A.: Technical Report of the Meteorological Research Institute, Japan, 64, 83 pp., 2011.

Zhang, P., Cheng, H., Edwards, R. L., Chen, F., Wang, Y., Yang, X., Liu, J., Tan, M., Wang, X., Liu, J., An, C., Dai, Z., Zhou, J., Zhang, D., Jia, J., Jin, L., and Johnson, K. R.: A test of climate, sun, and culture relationships from an 1810-year Chinese cave record, Science, 322, 940–942, 2008.

Zhou, T, Wu, B., Wen, X., Li, L., and Wang, B.: A fast version of LASG/IAP climate system model and its 1000-year control integration, Adv. Atmos. Sci., 25, 655–672, 2008.

Table 1. CMIP5/PMIP3 LM model simulations used, including key reference and definition of LIA and MCA periods in each model.

Model	MCA	LIA	Period (CE)	Reference
bcc-csm-1	1040–1130	1590–1790	851–2000	–
CCSM4	1110–1200	1710–1810	850–1850	Gent et al. (2001)
CSIRO-Mk3L-1–2	950–1050	1760–1850	851–2000	Phipps et al. (2011)
FGOALS-gl	1210–1270	1690–1820	1000–2000	Zhou et al. (2008)
FGOALS-s2	915–990	1710–1790	850–1850	Zhou et al. (2008)
HadCM3	1160–1250	1600–1700	801–2000	Schurer et al. (2013)
IPSL-CM5A-LR	910–950	1630–1710	850–1850	Dufresne et al. (2013)
MPI-ESM-P	1120–1220	1600–1680	850–1850	Raddatz eet al. (2007)
MRI-CGCM3	1130–1230	1510–1620	850–1849	Yukimoto et al. (2011)

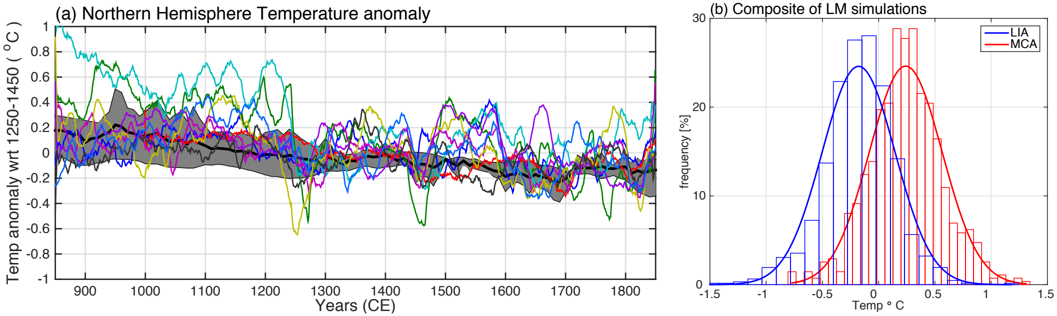

Figure 1. (a) Northern Hemisphere (north of 30° N) temperature anomaly evolution. Black line: mean on three reconstructions, grey envelope: maximum and minimum values of three reconstructions, colour lines: nine CMIP5/PMIP3 models considered in this study. **(b)** Distribution of temperatures during the Medieval Climate Anomaly (MCA, red curve) and Little Ice Age (LIA, blue curves), all with respect to the reference period 1250–1450 CE.

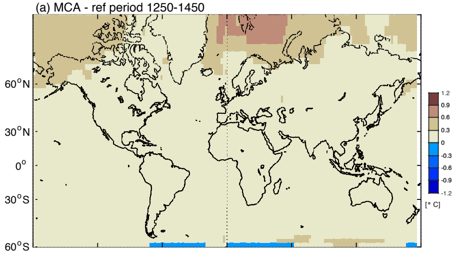
(a) MCA - ref period 1250-1450

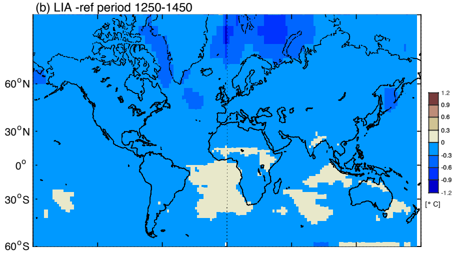
(b) LIA -ref period 1250-1450

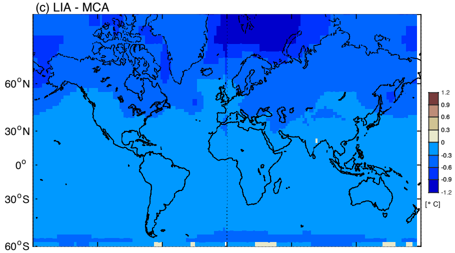
(c) LIA - MCA

Figure 2. Model mean annual mean temperatures. **(a)** Difference between MCA and reference period 1250–1450 CE, **(b)** difference between LIA and reference period, **(c)** LIA – MCA.

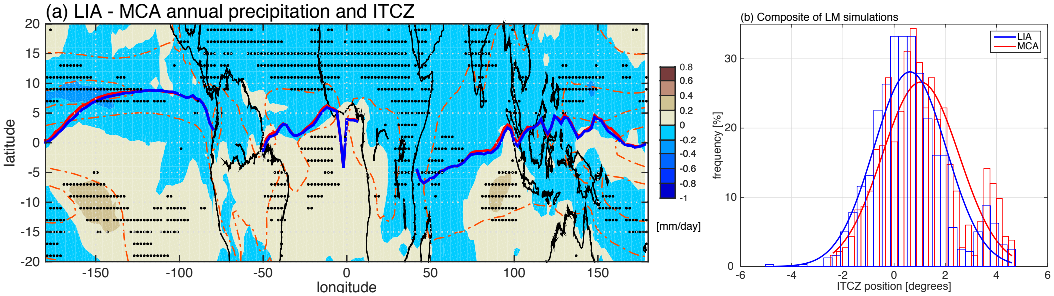

Figure 3. (a) Model mean annual mean LIA – MCA precipitation difference (colours), reference period precipitation (dashed orange lines, contours every 4 mm day^{-1}) and position of the oceanic Intertropical Convergence Zone (ITCZ) of MCA (red line) and LIA (blue line). Dots indicate grid-points where precipitation differences are significant (t test, $p < 0.05$). **(b)** Distribution of the zonal mean position [degrees] of the oceanic ITCZ in MCA (red curve) and LIA (blue curve).

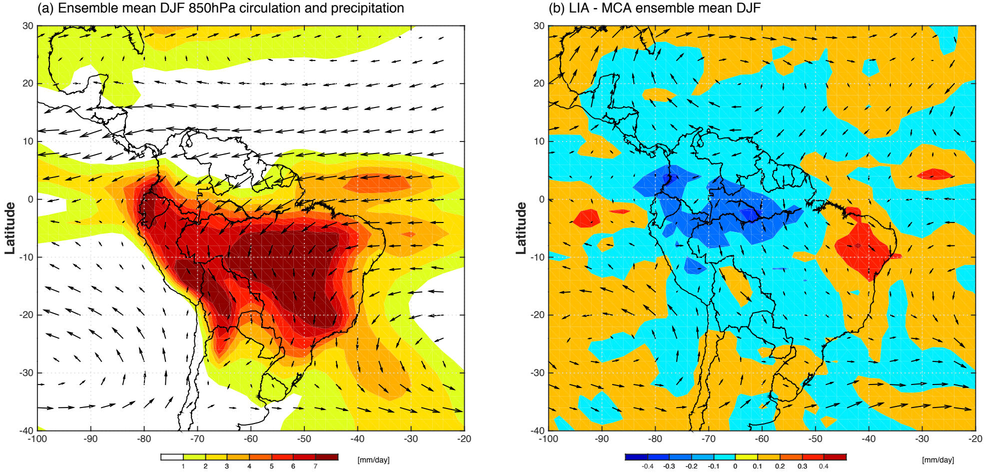

Figure 4. (a) Model mean December–January–February (DJF) 850 hPa winds (vectors) and precipitation (colours) for the reference period (1250–1450 CE). **(b)** DJF mean LIA – MCA winds (vectors) and precipitation difference (colours).

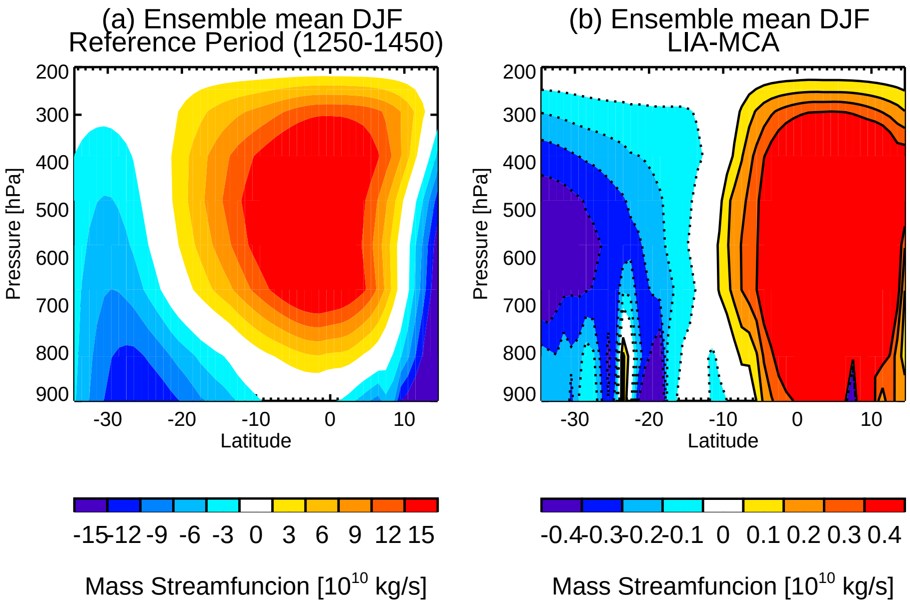

Figure 5. Model mean DJF meridional mass stream function over the region 80–30° W, depicting the regional Hadley Cell. **(a)** Climatology for reference period (1250–1450 CE), Red (blue) colours indicate clockwise (counterclockwise) circulation, **(b)** LIA – MCA.

Title Page
Abstract
Introduction
Conclusions
References
Tables
Figures
◀|
|▶
◀
▶
Back
Close
Full Screen / Esc
Printer-friendly Version
Interactive Discussion

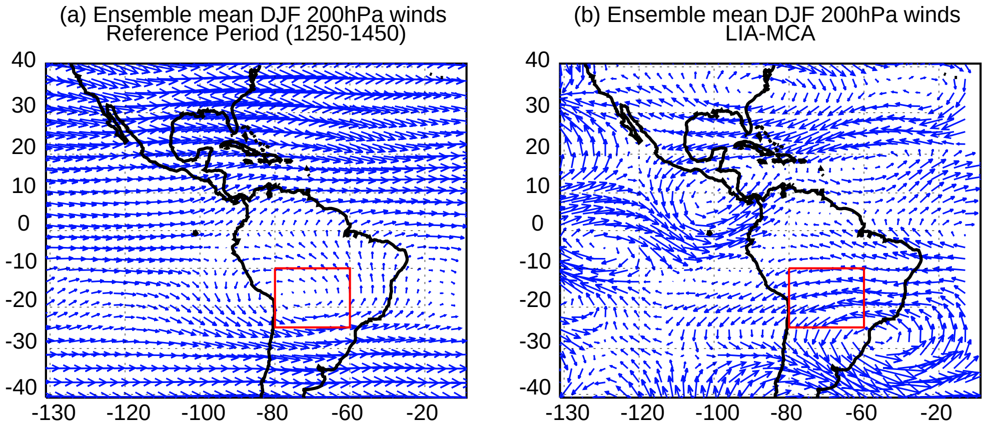

Figure 6. Model mean DJF circulation at 200 hPa. **(a)** Climatology for reference period (1250–1450 CE). **(b)** LIA – MCA differences. Red box represents the South American Monsoon System (SAMS) domain.

CPD

11, 5651–5681, 2015

Title Page
Abstract
Introduction
Conclusions
References
Tables
Figures
◀◀
▶▶
◀
▶
Back
Close
Full Screen / Esc
Printer-friendly Version
Interactive Discussion

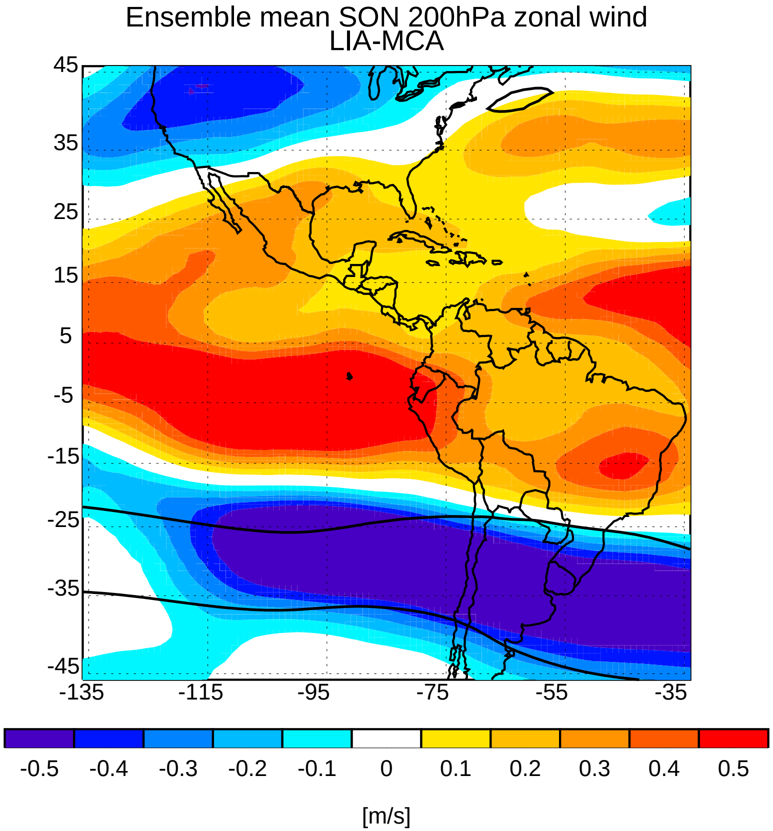

Figure 7. Model mean LIA – MCA 200 hPa zonal wind for September–October–November (SON). Black contour corresponds to the 30 m s^{-1} isotach of reference period zonal wind (1250–1450 CE).